Entanglement-Enabled Delayed-Choice Experiment

Florian Kaiser *et al.*

Science **338**, 637 (2012);
DOI: 10.1126/science.1226755

15. A. Zeilinger, G. Weihs, T. Jennewein, M. Aspelmeyer, *Nature* **446**, 342 (2007).
16. V. Jacques *et al.*, *Science* **315**, 966 (2007).
17. R. Ionicioiu, D. R. Terno, *Phys. Rev. Lett.* **107**, 230406 (2011).
18. P. J. Shadbolt *et al.*, *Nat. Photonics* **6**, 45 (2012).
19. S. S. Roy, A. Shukla, T. S. Mahesh, *Phys. Rev. A* **85**, 022109 (2012).
20. R. Auccaise *et al.*, *Phys. Rev. A* **85**, 032121 (2012).
21. J. S. Bell, *Physics* **1**, 195 (1964).
22. M. A. Nielsen, I. L. Chuang, *Quantum Computation and Quantum Information* (Cambridge Univ. Press, Cambridge, MA, 2000).
23. T. C. Ralph, N. K. Langford, T. B. Bell, A. G. White, *Phys. Rev. A* **65**, 062324 (2002).
24. H. F. Hofmann, S. Takeuchi, *Phys. Rev. A* **66**, 024308 (2002).
25. J. F. Clauser, M. Horne, A. Shimony, R. A. Holt, *Phys. Rev. Lett.* **23**, 880 (1969).
26. Materials and methods are available as supplementary materials on *Science* Online.
27. B. S. Cirel'son, *Lett. Math. Phys.* **4**, 93 (1980).
28. A. Aspect, J. Dalibard, G. Roger, *Phys. Rev. Lett.* **49**, 1804 (1982).
29. G. Weihs, T. Jennewein, C. Simon, H. Weinfurter, A. Zeilinger, *Phys. Rev. Lett.* **81**, 5039 (1998).
30. J.-S. Tang, Y.-L. Li, C.-F. Li, G.-C. Guo, *Nat. Photonics* **6**, 602 (2012).
31. T. Qureshi, *Quantum Phys.*, arXiv:1205.2207.
32. X.-s. Ma, *Quantum Phys.*, arXiv:1206.6578.
33. F. Kaiser, T. Coudreau, P. Milman, D. B. Ostrowsky, S. Tanzilli, *Science* **338**, 637 (2012).

Acknowledgments: We thank R. Ionicioiu, S. Pironio, T. Rudolph, N. Sangouard, and D. R. Terno for useful discussions, and acknowledge financial support from the UK Engineering and Physical Sciences Research Council (EPSRC), European Research Council (ERC), the Quantum Integrated Photonics (QUANTIP) project, A Toolbox for Photon Orbital Angular Momentum Technology (PHORBITECH) project, the Quantum InterfacES, SENsors, the Communication based on Entanglement (Q-ESSENCE) integrating project, Nokia, the Centre for Nanoscience and Quantum Information (NSQI), the Templeton Foundation, and the European Union Union Device-Independent Quantum Information Processing (DIQIP) project. J.L.O. and S.P. acknowledge a Royal Society Wolfson Merit Award. A.P. holds a Royal Academy of Engineering Research Fellowship.

Supplementary Materials

www.sciencemag.org/cgi/content/full/338/6107/634/DC1
Materials and Methods
Fig. S1

28 June 2012; accepted 18 September 2012
10.1126/science.1226719

Entanglement-Enabled Delayed-Choice Experiment

Florian Kaiser,[1] Thomas Coudreau,[2] Pérola Milman,[2,3] Daniel B. Ostrowsky,[1] Sébastien Tanzilli[1]*

Wave-particle complementarity is one of the most intriguing features of quantum physics. To emphasize this measurement apparatus–dependent nature, experiments have been performed in which the output beam splitter of a Mach-Zehnder interferometer is inserted or removed after a photon has already entered the device. A recent extension suggested using a quantum beam splitter at the interferometer's output; we achieve this using pairs of polarization-entangled photons. One photon is tested in the interferometer and is detected, whereas the other allows us to determine whether wave, particle, or intermediate behaviors have been observed. Furthermore, this experiment allows us to continuously morph the tested photon's behavior from wavelike to particle-like, which illustrates the inadequacy of a naive wave or particle description of light.

Although the predictions of quantum mechanics have been verified with marked precision, subtle questions arise when attempting to describe quantum phenomena in classical terms (*1*, *2*). For example, a single quantum object can behave as a wave or as a particle. This concept is illustrated by Bohr's complementarity principle (*3*) which states that, depending on the measurement apparatus, either wave or particle behavior is observed (*4*, *5*). This is demonstrated by sending single photons into a Mach-Zehnder interferometer (MZI) followed by two detectors (Fig. 1A) (*6*). If the MZI is closed [that is, if the paths of the interferometer are recombined at the output beam splitter (BS_2)], the probabilities for a photon to exit at detectors D_a and D_b depend on the phase difference θ between the two arms. The which-path information remains unknown, and wavelike intensity interference patterns are observed (Fig. 1B). On the other hand, if the MZI is open (i.e., if BS_2 is removed), each photon's path can be known, and consequently, no interference occurs. Particle behavior is said to be observed, and the detection probabilities at D_a and D_b are equal to ½, independent of the value of θ (Fig. 1C). In other words, these two different configurations—BS_2 present or absent—give different experimental results. Recently, Jacques *et al.* have shown that, even when performing Wheeler's original gedanken experiment (*7*) in which the configuration for BS_2 is chosen only after the photon has passed the entrance beam splitter BS_1, Bohr's complementarity principle is still obeyed (*8*). Intermediate cases, in which BS_2 is only partially present, have been considered in theory and led to a more general description of Bohr's complementarity principle expressed by an inequality limiting the simultaneously available amount of interference (signature of wavelike behavior) and which-path information (particle-like behavior) (*9*, *10*). This inequality has also been confirmed experimentally in delayed-choice configurations (*11*, *12*).

We take Wheeler's experiment one step further by replacing the output beam splitter by a quantum beam splitter (QBS), as theoretically proposed of late (*13*, *14*). In our experiment (Fig. 2), we exploit polarization entanglement as a resource for two reasons. First, doing so permits implementing the QBS. Second, it allows us to use one of the entangled photons as a test photon sent to the interferometer and the other one as a corroborative photon. Here, as opposed to previous experiments (*8*, *11*), the state of the interferometer remains unknown, as does the wave or particle behavior of the test photon, until we detect the corroborative photon. By continuously modifying the type of measurement performed on the corroborative photon, we can morph the test photon from wave to particle behavior, even after the test photon was detected. To exclude interpretations based on either mixed states, associated with preexisting state information (*15*), or potential communication between the two photons, the presence of entanglement is verified via the violation of the Bell inequalities with a spacelike separation (*16*–*18*).

The QBS is based on the idea that when a photon in an arbitrary polarization state enters an interferometer that is open for $|H\rangle$ (horizontally polarized) and closed for $|V\rangle$ (vertically polarized) photons, the states of the interferometer and the photon become correlated. Our apparatus, shown in the right-hand side of Fig. 2 and detailed in fig. S1, therefore reveals a particle behavior for the $|H\rangle$ component of the photon state and a wave behavior for the $|V\rangle$ component. Note that such an experiment has been realized with the use of single photons prepared in a coherent superposition of $|H\rangle$ and $|V\rangle$ (*12*). However, we take this idea a step further by achieving genuine quantum behavior for the output beam splitter by exploiting an intrinsically quantum resource, entanglement. This allows us to entangle the quantum beam splitter and test photon system with the corroborative photon. Thus, measurement of the corroborative photon enables us to project the test photon–QBS system into an arbitrary coherent wave-particle superposition, which is a purely quantum object. In other words, our QBS is measured by another quantum object, which projects it into a particular superposition of present and absent states. More precisely, we use as a test photon one of the photons from the maximally polarization-entangled Bell state $|\Phi^+\rangle = \frac{1}{\sqrt{2}}(c_H^\dagger t_H^\dagger + c_V^\dagger t_V^\dagger)|vac\rangle$, produced at the wavelength of 1560 nm using the source described in (*19*). Here, using the notation of Fig. 2,

[1]Laboratoire de Physique de la Matière Condensée, CNRS UMR 7336, Université de Nice–Sophia Antipolis, Parc Valrose, 06108 Nice Cedex 2, France. [2]Laboratoire Matériaux et Phénomènes Quantiques, Université Paris Diderot, Sorbonne Paris Cité, CNRS, UMR 7162, 75013 Paris, France. [3]Institut de Sciences Moléculaires d'Orsay (CNRS) Bâtiment 210, Université Paris Sud 11, Campus d'Orsay, 91405, Orsay Cedex, France.

*To whom correspondence should be addressed. E-mail: sebastien.tanzilli@unice.fr

$c_H^\dagger(t_H^\dagger)$ and $c_V^\dagger(t_V^\dagger)$ represent creation operators for horizontally and vertically polarized photonic modes, respectively, propagating toward the corroborative (test) photon apparatus. Moreover, $|vac\rangle$ represents the vacuum state. Using an entangled state of this form ensures maximum randomness of the input polarization state of the test photon (t), which enters an MZI with a QBS for the output beam splitter.

The actual QBS device is made up of two components. The first is a polarization-dependent beam splitter (PDBS) that shows close to 100% reflection for horizontally polarized photons and provides an ordinary 50/50 splitting ratio for the vertically polarized photons. The PDBS is realized using a combination of standard bulk optical components, as described in supplementary text S1. The whole state after the PDBS reads

$$|\Psi\rangle = \frac{1}{2}\left(c_H^\dagger(-e^{i\theta}a_H^\dagger + ib_H^\dagger) + \frac{1}{\sqrt{2}}c_V^\dagger(b_V^\dagger(i + ie^{i\theta}) + a_V^\dagger(1 - e^{i\theta}))\right)|vac\rangle \quad (1)$$

Here, θ is an adjustable phase shift in the interferometer, i is the complex imaginary unit, and $a_H^\dagger$, $a_V^\dagger$, $b_H^\dagger$, and $b_V^\dagger$ symbolize creation operators for test photons propagating toward PBS_1 and PBS_2, respectively. At this point, each polarization state of the test photon is associated with one of the two complementary types of behaviors, wave and particle.

The second stage consists of polarizing beam splitters (PBS_1 and PBS_2) oriented at 45° to the $\{H, V\}$ basis, which permits the erasure of all polarization information that potentially existed at the PDBS output (*4*, *5*, *20*). Equation 1 becomes

$$|\Psi\rangle = \frac{1}{\sqrt{2}}(c_H^\dagger[particle]^\dagger + c_V^\dagger[wave]^\dagger)|vac\rangle \quad (2)$$

with

$$[particle]^\dagger = \frac{1}{2}(-e^{i\theta}(a'^\dagger + a''^\dagger) + i(b'^\dagger + b''^\dagger)) \quad (3)$$

and

$$[wave]^\dagger = \frac{1}{2\sqrt{2}}((1 - e^{i\theta})(-a'^\dagger + a''^\dagger) + i(1 + e^{i\theta})(-b'^\dagger + b''^\dagger)) \quad (4)$$

Here, the creation operators $a'^\dagger$, $a''^\dagger$, $b'^\dagger$, and $b''^\dagger$ denote photons propagating toward detectors $D_{a'}$, $D_{a''}$, $D_{b'}$, and $D_{b''}$, respectively. Consequently, the only way of knowing if wave or particle behavior was observed is by examining the corroborative photon.

The corroborative photon measurement apparatus, as shown on the left-hand side of Fig. 2, consists of two stages. The first is an electro-optic phase modulator that allows us to rotate the

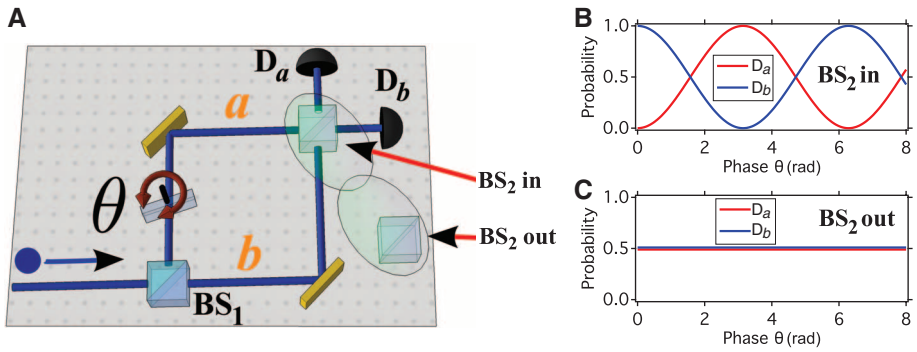

Fig. 1. (**A**) Wheeler's gedanken experiment using an MZI. The device consists of two beam splitters, BS_1 and BS_2; a glass plate introducing a phase shift θ; and two detectors, D_a and D_b, at its output. (**B**) Simulated photon-detection probabilities at detectors D_a and D_b as a function of the phase θ. The sinusoidal oscillations are related to unknown path information and, therefore, to single-photon interference, which is a wavelike phenomenon. rad, radians. (**C**) Detection probabilities without BS_2. No interference is observed, which is the signature of particle behavior.

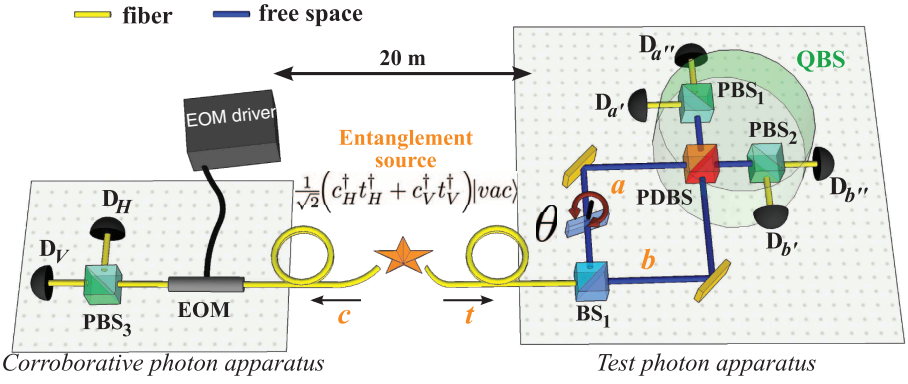

Fig. 2. Experimental setup. Via a single-mode optical fiber, a source of polarization-entangled photons [λ = 1560 nm, see (*13*) for more details] sends one photon (t) to a QBS apparatus, which is an open (or closed) MZI for horizontally (or vertically) polarized photons. This is enabled by the use of a PDBS. The second photon (c) of the entangled state is sent to another laboratory 20 m away (spacelike separation) and used as a "corroborative" photon, which allows us to determine whether we observed wavelike, particle-like, or both behaviors of photon t. EOM, electro-optic phase modulator.

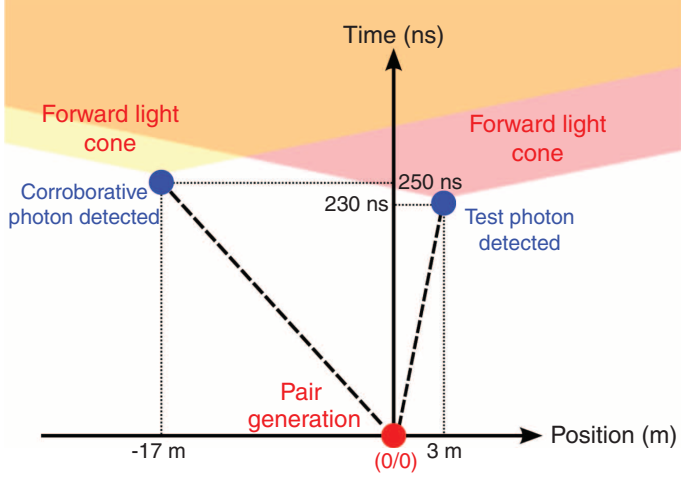

Fig. 3. Space-time diagram of the experimental apparatus. The paired photons are said to be generated and separated at the origin (0/0). The test photon travels ~50 m in an optical fiber before entering the QBS apparatus, which is located in the same laboratory as the entangled photon pair source. The corroborative photon is sent through a 55-m fiber to another laboratory. The corroborative and test photon apparatuses are physically separated by 20 m. The corroborative photon was measured 20 ns after the test photon was detected, thus revealing the MZI configuration in a delayed fashion. The forward light cones from both photon-detection events do not overlap, demonstrating that spacelike separation is achieved. In other words, no causal connection between these events can be established.

polarization state of the corroborative photon by an angle α. From Eqs. 2 to 4, we now have

$$|\Psi\rangle = \frac{1}{\sqrt{2}}\left(c_H^\dagger(\cos\alpha[particle]^\dagger - \sin\alpha[wave]^\dagger) + c_V^\dagger\left(\cos\alpha[wave]^\dagger + \sin\alpha[particle]^\dagger\right)\right)|vac\rangle \quad (5)$$

After passing PBS_3, which is oriented on the {*H*, *V*} axis, the corroborative photon is transmitted (|H⟩) or reflected (|V⟩). This projects the test photon into a state defined by the terms in the parentheses of Eq. 5. Therefore, the firing of detector D_H indicates that the test photon is in the state $\cos\alpha[particle]^\dagger - \sin\alpha[wave]^\dagger$, whereas the firing of D_V shows that it is in the state $\cos\alpha[wave]^\dagger + \sin\alpha[particle]^\dagger$. By choosing $0 < \alpha < 90°$, we obtain a continuous morphing between wave and particle behavior. The expected intensity correlations, given by the coincidence count probability between detectors D_H (corroborative) and $[D_{b'} \oplus D_{b''}]$ (test), where ⊕ denotes an exclusive OR (XOR) gate, are

$$I_{H,b}(\theta,\alpha) = \cos^2\frac{\theta}{2}\sin^2\alpha + \frac{1}{2}\cos^2\alpha \quad (6)$$

Note that the correlations between detectors D_V and $[D_{a'} \oplus D_{a''}]$ follow the same function. On the contrary, the complementary intensity correlations (that is, correlations between detectors D_H and $[D_{a'} \oplus D_{a''}]$ or between D_V and $[D_{b'} \oplus D_{b''}]$) are given by $1 - I_{H,b}(\theta,\alpha)$. The use of XOR gates permits counting the photons from both outputs of each quantum eraser (PBS_1 or PBS_2), and reaching an average coincidence rate of 70 s^{-1} for each of them. Note that Eq. 6 does not depend on the relative detection times of the two photons. In the experiment reported here, the detection of the corroborative photon is delayed until after the detection of the test photon. This is ensured by inserting an extra 5-m length of optical fiber in the path of the corroborative photon (*c*). In this case, for each of the four correlation functions mentioned above, the configuration of the interferometer remains undetermined, even after the test photon has been detected. In other words, there is no information available yet from the corroborative photon that could influence the behavior of the test photon. Furthermore, a space-time analysis shows that no classical communication can be established between the photon-detection events, as they have spacelike separation (Fig. 3).

We now measure the correlations between detectors D_H and $[D_{b'} \oplus D_{b''}]$ via counting coincidence events on the corresponding single-photon detectors (InGaAs avalanche photodiodes). As shown in Fig. 4A, the experimentally measured results are in near-perfect agreement with the theoretical predictions of Eq. 6. For the angle $\alpha = 0°$, $I_{H,b}(\theta,0)$ is independent of the phase θ, as predicted for particle-like behavior. Setting $\alpha = 90°$ results in sinusoidal intensity oscillations as a function of θ, which corresponds to wavelike behavior. For $0° < \alpha < 90°$, a continuous transition from wave to particle behavior is observed, expressed by the continually reducing fringe visibility. As outlined in (*9*, *10*), a generalization of Bohr's complementarity principle implies the interference fringe visibility *V* and the path distinguishability *D*, also called the which-way information, to be limited by the following inequality

$$V^2 + D^2 \leq 1 \quad (7)$$

The experimental measurement of these two quantities is described in supplementary text S2 (*11*, *12*). Figure 4B shows the obtained results for V^2, D^2, and $V^2 + D^2$ as a function of the angle α. With our experimental data, Eq. 7 is confirmed for all angles of α.

To prove the existence of a coherent quantum superposition of wave and particle behavior of the

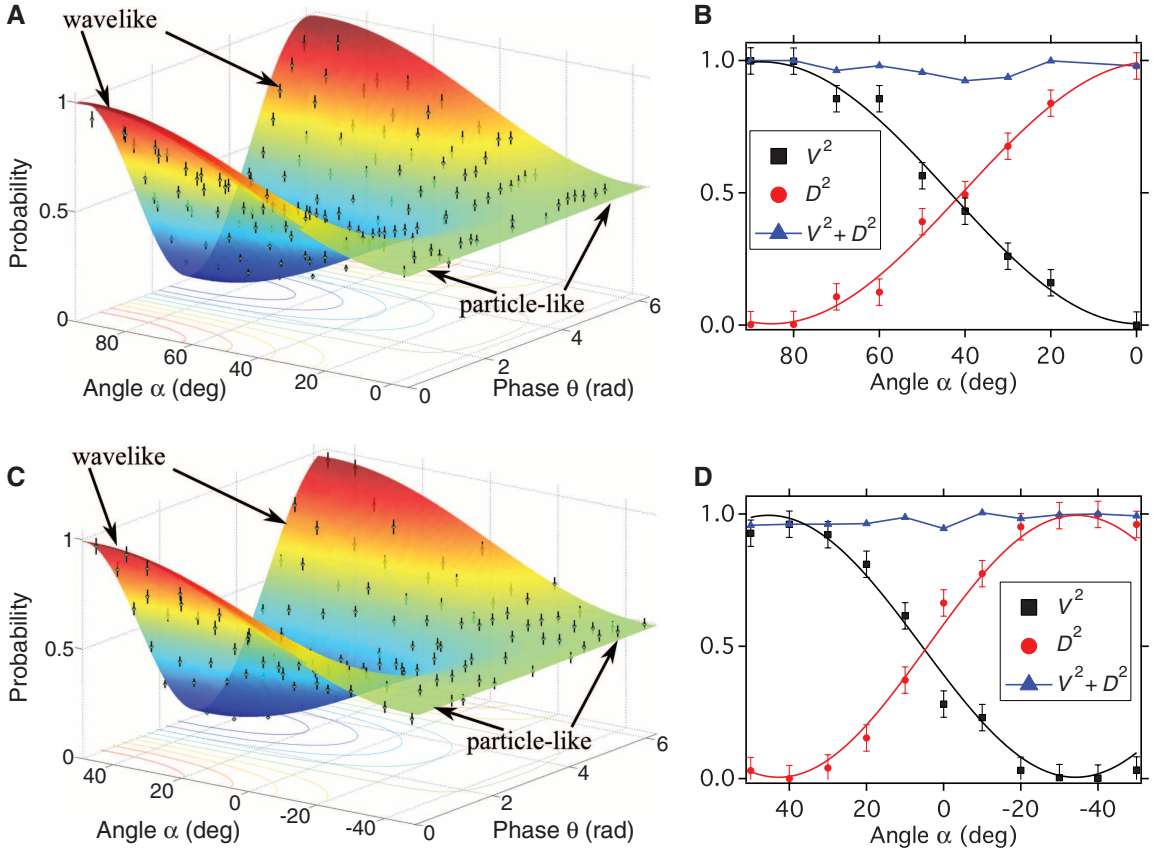

Fig. 4. Experimental results for the quantum delayed-choice experiment. (**A** and **C**) Plots of the intensity correlations, $I_{H,b}(\theta,\alpha)$, as defined by Eq. 6, expressed as the probability of a coincidence event between detectors D_H and $[D_{b'} \oplus D_{b''}]$ as a function of α and θ. Dots and associated vertical lines represent experimental data points and their corresponding standard deviations. Wave-particle morphing is observed for the natural {*H*, *V*} basis (**A**), as well as for the complementary {*D*, *A*} basis (**C**). The colored surfaces in these graphs represent the best fits to the experimental data using Eq. 6. Note that the result obtained for the {*D*, *A*} basis is essential because it represents the signature of the entangled state, proving the correct implementation of the desired quantum beam-splitting effect. We obtain average coincidence rates of 350 events per 5 s. The noise contribution, on the order of three events per 5 s, has not been subtracted. (**B** and **D**) Plots and related sinusoidal fits (solid lines) of the fringe visibility *V* (black) and path distinguishability *D* (red) as a function of the angle α. For all angles, we verify $V^2 + D^2 \leq 1$, as predicted by Eq. 7; the blue solid line serves as a guide for the eyes. Note that the same experimental results would be obtained if the timing order of the measurements of the test and corroborative photons were inverted (*26*). Error bars indicate the relative uncertainty obtained in the photon-counting measurements.

test photon created by the detection of the corroborative photon, the presence of entanglement must be verified (*16*, *21*). Note that several recent works did not do this; therefore, the presence of a QBS has not been proven unambiguously (*22*, *23*). In our realization, entanglement is proven by performing the same experiment as before, but using the complementary analysis basis, namely the diagonal basis $\{D, A\}$. Now, the initial quantum state is rotated by 45°—i.e., $\frac{1}{\sqrt{2}}(c_V^\dagger t_V^\dagger + c_H^\dagger t_H^\dagger)|vac\rangle \rightarrow \frac{1}{\sqrt{2}}(c_D^\dagger t_D^\dagger + c_A^\dagger t_A^\dagger)|vac\rangle$—where D and A symbolize diagonally and antidiagonally polarized photon contributions, respectively. In this configuration, every single photon is unpredictably subjected to a closed or open Mach-Zehnder configuration by the PDBS. In this case, as opposed to the experiment in the $\{H, V\}$ basis, if a statistical mixture was analyzed instead of an entangled state, no correlations should be observed when measuring $I_{H,b}(\theta,\alpha)$. However, the strong correlations shown in Fig. 4C exclude a statistical mixture and are in good agreement with the theoretical predictions of Eq. 6. This emphasizes that wave and particle behavior coexist simultaneously for the entire range $0° < \alpha < 90°$ in the $\{H, V\}$ basis and for $-45° < \alpha < 45°$ in the $\{D, A\}$ basis. Figure 4D shows the measurements for V^2, D^2, and $V^2 + D^2$ as a function of α and confirms the upper limits imposed by Eq. 7. The quality of the entangled state is measured via the Bell parameter S, which is deduced from the phase oscillation visibilities at $\alpha = 90°$ in the $\{H, V\}$ basis and $\alpha = 45°$ in the $\{D, A\}$ basis. We obtain $S = 2.77 \pm 0.07$, which is very close to the optimal value of $2\sqrt{2}$ attained with maximally entangled states and is 11 standard deviations above the classical/quantum boundary $S = 2$ (*16*, *21*).

The detection loophole remains open in our experiment, because some of the initial entangled photons are lost during their propagation in the fiber or bulk channels or are not detected by the single-photon detectors that show nonunit quantum detection efficiencies (*24*). Therefore, we make the reasonable assumption that the detected photons represent a faithful sample (*17*).

In conclusion, we have carried out a quantum delayed-choice experiment, enabled by polarization-entangled photons and the associated property of nonlocality. We used an MZI in which the output beam splitter has been replaced by its quantum analog (i.e., a beam splitter in a coherent superposition of being present and absent). In this configuration, we observed that single photons can behave as waves and as particles in the same experiment, meaning that the simple view of photons being either waves or particles is refuted. We experimentally excluded interpretations based on local hidden variables and/or information exchange between the photon and the quantum beam splitter. The state of the quantum beam splitter is determined by the detection of the corroborative photon. We have, therefore, demonstrated delayed interference between wave and particle behavior, which underlines the subtleness of Bohr's complementarity principle.

We note that, parallel to this work, Peruzzo *et al.* realized another version of a quantum delayed-choice experiment based on entangled photons (*25*).

References and Notes

1. E. Schrödinger, *Naturwissenschaften* **23**, 807 (1935).
2. G. Greenstein, A. Zajonc, *The Quantum Challenge: Modern Research on the Foundations of Quantum Mechanics* (Jones and Bertlett Publishers, Sudbury, MA, 2006).
3. N. Bohr, in *Quantum Theory and Measurement*, J. A. Wheeler, W. H. Zurek, Eds. (Princeton Univ. Press, Princeton, NJ, 1984), p. 949.
4. Y.-H. Kim, R. Yu, S. P. Kulik, Y. Shih, M. O. Scully, *Phys. Rev. Lett.* **84**, 1 (2000).
5. S. P. Walborn, M. O. Terra Cunha, S. Pádua, C. H. Monken, *Phys. Rev. A* **65**, 033818 (2002).
6. P. Grangier, G. Roger, A. Aspect, *Europhys. Lett.* **1**, 173 (1986).
7. J. A. Wheeler, in *Quantum Theory and Measurement*, J. A. Wheeler, W. H. Zurek, Eds. (Princeton Univ. Press, Princeton, NJ, 1984), pp. 182–213.
8. V. Jacques *et al.*, *Science* **315**, 966 (2007).
9. W. K. Wootters, W. H. Zurek, *Phys. Rev. D* **19**, 473 (1979).
10. B.-G. Englert, *Phys. Rev. Lett.* **77**, 2154 (1996).
11. V. Jacques *et al.*, *Phys. Rev. Lett.* **100**, 220402 (2008).
12. J.-S. Tang *et al.*, *Nat. Photonics* **6**, 602 (2012).
13. R. Ionicioiu, D. R. Terno, *Phys. Rev. Lett.* **107**, 230406 (2011).
14. M. Schirber, *Physics* **4**, 102 (2011).
15. A. Einstein, B. Podolsky, N. Rosen, *Phys. Rev.* **47**, 777 (1935).
16. J. S. Bell, *Physics* **1**, 195 (1964).
17. A. Aspect, J. Dalibard, G. Roger, *Phys. Rev. Lett.* **49**, 1804 (1982).
18. G. Weihs, T. Jennewein, C. Simon, H. Weinfurter, A. Zeilinger, *Phys. Rev. Lett.* **81**, 5039 (1998).
19. F. Kaiser, A. Issautier, O. Alibart, A. Martin, S. Tanzilli, *Phys. Rev. Lett.* **75**, 3034 (1995).
21. J. F. Clauser, M. A. Horne, A. Shimony, R. A. Holt, *Phys. Rev. Lett.* **23**, 880 (1969).
22. S. S. Roy, A. Shukla, T. S. Mahesh, *Phys. Rev. A* **85**, 022109 (2012).
23. R. Auccaise *et al.*, *Phys. Rev. A* **85**, 032121 (2012).
24. J. F. Clauser, M. A. Horne, *Phys. Rev. D Part. Fields* **10**, 526 (1974).
25. A. Peruzzo, P. Shadbolt, N. Brunner, S. Popescu, J. L. O'Brien, *Science* **338**, 634 (2012).
26. X.-S. Ma *et al.*, *Nat. Phys.* **8**, 480 (2012).

Acknowledgments: We thank L. A. Ngah for his help on data acquisition and O. Alibart for fruitful discussions. This work was supported by the CNRS, l'Université de Nice–Sophia Antipolis, l'Agence Nationale de la Recherche for the "e-QUANET" project (grant ANR-09-BLAN-0333-01), the European ICT-2009.8.0 FET open program for the "QUANTIP" project (grant 244026), le Ministère de l'Enseignement Supérieur et de la Recherche, la Fondation iXCore pour la Recherche, and le Conseil Régional PACA for the "QUANET" project in the exploratory call.

Supplementary Materials

www.sciencemag.org/cgi/content/full/338/6107/637/DC1
Supplementary Text
Fig. S1

29 June 2012; accepted 18 September 2012
10.1126/science.1226755

Quantum Entanglement of High Angular Momenta

Robert Fickler,[1,2]* Radek Lapkiewicz,[1,2] William N. Plick,[1,2] Mario Krenn,[1,2] Christoph Schaeff,[1,2] Sven Ramelow,[1,2] Anton Zeilinger[1,2,3]*

Single photons with helical phase structures may carry a quantized amount of orbital angular momentum (OAM), and their entanglement is important for quantum information science and fundamental tests of quantum theory. Because there is no theoretical upper limit on how many quanta of OAM a single photon can carry, it is possible to create entanglement between two particles with an arbitrarily high difference in quantum number. By transferring polarization entanglement to OAM with an interferometric scheme, we generate and verify entanglement between two photons differing by 600 in quantum number. The only restrictive factors toward higher numbers are current technical limitations. We also experimentally demonstrate that the entanglement of very high OAM can improve the sensitivity of angular resolution in remote sensing.

Quantum entanglement—the nonclassical phenomenon of joint measurements of at least two separate systems showing stronger correlations than classically explainable (*1*, *2*)—is widely considered one of the quintessential features of quantum theory. Since its discovery and first experimental demonstration (*3*), photon entanglement has been shown in various degrees of freedom (*4*–*7*). In the field of photonic quantum optics, studies of the orbital angular momentum (OAM) of light have been productive. The natural solutions of the paraxial wave equation in cylindrical coordinates, Laguerre-Gauss modes, have a helical phase dependence that leads to a vortex or phase singularity and thus zero intensity along the beam axis. These Laguerre-Gauss modes carry an OAM that can take any integer value (*8*). Entanglement of OAM of photons (*5*) has led to many novel insights and applications in quantum foundations and quantum information—for example, qutrit quantum com-

[1]Quantum Optics, Quantum Nanophysics, Quantum Information, University of Vienna, Vienna A-1090, Austria. [2]Institute for Quantum Optics and Quantum Information, Austrian Academy of Science, Vienna A-1090, Austria. [3]Vienna Center for Quantum Science and Technology, Faculty of Physics, University of Vienna, Vienna A-1090, Austria.

*To whom correspondence should be addressed. E-mail: robert.fickler@univie.ac.at (R.F.); anton.zeilinger@univie.ac.at (A.Z.)